RAA 2021 Vol. **21** No. **2**, 27(7pp) doi: 10.1088/1674-4527/21/2/27

http://www.raa-journal.org *http://iopscience.iop.org/raa*

***R**esearch in*
***A**stronomy and*
***A**strophysics*

Orbital period correction and light curve modeling of the W-subtype shallow contact binary OW Leo

Xiao Zhou[1,2,3] and Sheng-Bang Qian[1,2,3,4]

[1] Yunnan Observatories, Chinese Academy of Sciences (CAS), Kunming 650216, China; *zhouxiaophy@ynao.ac.cn*
[2] Key Laboratory of the Structure and Evolution of Celestial Objects, Chinese Academy of Sciences, Kunming 650216, China
[3] Center for Astronomical Mega-Science, Chinese Academy of Sciences, Beijing 100101, China
[4] University of the Chinese Academy of Sciences, Beijing 100049, China

Received 2020 July 8; accepted 2020 July 27

Abstract Orbital period and multi-color light curves' investigation of OW Leo are presented for the first time. The orbital period of OW Leo is corrected from $P = 0.325545$ days to $P = 0.32554052$ days in our work, and the observational data from the All-Sky Automated Survey for SuperNovae (ASAS-SN) are used to test the newly determined orbital period. Then, the phased light curves are calculated with the new period and the Wilson-Devinney program is applied to model the light curves, which reveal that OW Leo is a W-subtype shallow contact binary system ($q = 3.05$, $f = 12.8\,\%$). The absolute physical parameters of the two component stars are estimated to be $M_1 = 0.31(1)M_\odot$, $M_2 = 0.95(3)M_\odot$, $R_1 = 0.63(1)R_\odot$, $R_2 = 1.04(1)R_\odot$, $L_1 = 0.43(1)L_\odot$ and $L_2 = 1.01(2)L_\odot$. The evolutionary status shows that the more massive star is less evolved than the less massive star. OW Leo has very low metal abundance, which means its formation and evolution are hardly influenced by any additional component. It is formed from an initially detached binary system through nuclear evolution and angular momentum loss via magnetic braking, and has passed a very long time of main sequence evolution.

Key words: techniques: photometric — binaries: eclipsing — stars: evolution

1 INTRODUCTION

Contact binaries, both inside and outside our Galaxy, have been proved to be powerful tools for studying a wide spectrum of astrophysical problems. They usually consist of F, G and K type stars and the component stars are embedded in a common envelope. Due to the strong interactions between the component stars, the formation and evolution scenario for contact binaries are entirely and totally different from those of single stars, and still remain to be an open issue. A few years ago, many contact binaries were observed by the photometric method. However, only very few targets have spectral information due to the low efficiency of spectroscopic observations. Owe to the Large Sky Area Multi-Object Fibre Spectroscopic Telescope (LAMOST) (Cui et al. 2012; Zhao et al. 2012), hundreds of thousands of contact binaries are provided with stellar atmospheric parameters, which makes it a better time to investigate contact binaries (Qian et al. 2017, 2018).

OW Leo, also named GSC 01443-00087 or NSVS 10352593, is a newly reported EW-type binary (Diethelm 2010). Its period was given as $P = 0.325545$ days in the International Variable Star Index (VSX) (Watson et al. 2006). The binary system was observed by the LAMOST project for two times, which were on 2013 March 24 and 2018 February 6. The low resolution spectra gave out two sets of stellar atmospheric parameters, which were listed in Table 1. There is no radial velocity curve published for the target and its light curves have not been analysed yet. In the present work, we will state our photometric observation on OW Leo in Section 2. Then, all available mid-eclipse times are gathered to investigate the orbital period changes of OW Leo in Section 3, and our observational light curves and the light curve from All-Sky Automated Survey for SuperNovae (ASAS-SN) are modeled to obtain its physical parameters in Section 4. Finally, the formation and evolution theories of OW Leo are discussed in Section 5.

Table 1 Stellar Atmospheric Parameters of OW Leo

T (K)	log (g)	[Fe/H]	Date
5605	4.131	–0.734	2013 March 24
5724	4.250	–0.606	2018 February 6

Table 2 Coordinates and V Band Magnitudes

Target	α_{2000}	δ_{2000}	$V_{\rm mag}$
OW Leo	$11^{\rm h}52^{\rm m}13.59^{\rm s}$	$+18°58'55.0''$	12.84
UCAC4 546–051376	$11^{\rm h}52^{\rm m}39.70^{\rm s}$	$+19°03'00.2''$	12.12
UCAC4 546–051360	$11^{\rm h}51^{\rm m}50.00^{\rm s}$	$+19°04'01.1''$	13.98

Table 3 New CCD Times of Mid-eclipse Times

JD (Hel.)	Error (d)	p/s	Filter	Date
2458488.3337	$\pm$0.0002	p	$B\ V\ R_C\ I_C$	2019 January 5
2458491.4265	$\pm$0.0002	s	$B\ V\ R_C\ I_C$	2019 January 8

2 OBSERVATIONS AND DATA REDUCTION

The multi-color light curves of OW Leo were obtained on 2019 January 5 and 8 with the Xinglong 85cm optical telescope of National Astronomical Observatories, Chinese Academy of Sciences. The telescope was equipped with a 2K $\times$ 2K CCD Camera, and its field of view (FOV) was 32.8 square arc-minutes (Zhou et al. 2009; Zhang et al. 2018b). Four filters (B, V, R_C and I_C) from Johnson-Cousins' filters systems were chosen for the observations and the observational images were processed with the Image Reduction and Analysis Facility (IRAF) (Tody 1986). UCAC4 546-051376 and UCAC4 546-051360 in the same field of view were chosen as the Comparison (C) star and Check (Ch) star since we used the differential photometry method to obtain the light variations of OW Leo. Their coordinates in J2000.0 epoch and magnitudes in V band are listed in Table 2. Finally, we obtained the light variations of OW Leo and the observational light curves were plotted in Figure 1.

As shown in Figure 1, we got the primary minimum (left of Fig. 1) and secondary minimum (right of Fig. 1) of the eclipsing binary system. Then, parabola fit was applied on the observed light minima curves and the mid-eclipse times were determined, which were listed in Table 3.

3 ORBITAL PERIOD INVESTIGATION

Orbital period variations are quite common among close binary systems due to the possible angular momentum loss (ALM) from binary systems or mass transfer between the primary or secondary stars (Zhang et al. 2018a; Liu et al. 2018). Thus, the $O-C$ method was widely used in correcting orbital period or calculating orbital period variations of close binaries (Pi et al. 2017; He & Wang 2019). For analysis the orbital period of OW Leo, all available mid-eclipse times are gathered and listed Table 4. The $O-C$ values listed in Column (4) of Table 4 are calculated with the linear equation:

$$\mathrm{Min}.I(\mathrm{HJD}) = 2453175.509 + 0^d.325545 \times E. \quad (1)$$

As displayed in Figure 2, linear fit is performed on the observed $O-C$ curve, which means the orbital period of OW Leo should be corrected from 0.325545 days to 0.32554052 days. The new ephemeris is determined to be:

$$\begin{aligned}\mathrm{Min}.I = {} & 2453175.5153(\pm0.0002) \\ & + 0^d.32554052(\pm0.00000002) \times E\end{aligned} \quad (2)$$

Table 4 Mid-eclipse Times and $O-C$ Values of OW Leo

JD(Hel.) (2400000+)	p/s	Epoch	$O-C$ (d)	Error (d)	Ref.
53175.509	p	0	0		1
55269.7211	p	6433	–0.0189	0.0005	1
55604.8643	s	7462.5	–0.0243	0.0006	2
55973.8650	p	8596	–0.0288	0.0007	3
56041.7390	s	8804.5	–0.0310	0.0021	3
58488.3337	p	16320	–0.0697	0.0002	4
58491.4265	s	16329.5	–0.0696	0.0001	4

Reference: (1) Diethelm (2010); (2) Diethelm (2011); (3) Diethelm (2012); (4) the present work.
Column (1): the observed mid-eclipse times in HJD; Col. (2): primary (p) or secondary (s) light minima; Col. (3): cycle numbers calculated from Eq. 1; Col. (4): the calculated $O-C$ values based on Eq. (1); Col. (5): observational errors; Col. (6): the references.

Table 5 Photometric Results of OW Leo

Parameter	Value
T_2(K)	5665(assumed)
q (M_2/M_1)	3.05($\pm$0.05)
$i(^\circ)$	68.2($\pm$0.1)
T_1(K)	5885($\pm$5)
ΔT(K)	220($\pm$5)
$L_1/(L_1+L_2)\,(B)$	0.3169($\pm$0.0008)
$L_1/(L_1+L_2)\,(V)$	0.3041($\pm$0.0006)
$L_1/(L_1+L_2)\,(R_c)$	0.2981($\pm$0.0005)
$L_1/(L_1+L_2)\,(I_c)$	0.2937($\pm$0.0005)
r_1(pole)	0.2731($\pm$0.0002)
r_1(side)	0.2852($\pm$0.0003)
r_1(back)	0.3220($\pm$0.0005)
r_2(pole)	0.4540($\pm$0.0002)
r_2(side)	0.4883($\pm$0.0003)
r_2(back)	0.5157($\pm$0.0004)
$\Omega_1 = \Omega_2$	6.603($\pm$0.003)
f	12.8 %($\pm$0.5 %)
$\Sigma\omega(O-C)^2$	0.0018

Table 6 Absolute Parameters of the Component Stars in OW Leo

Parameter	Primary star	Secondary star
M	$0.31(\pm0.01)M_\odot$	$0.95(\pm0.03)M_\odot$
R	$0.63(\pm0.01)R_\odot$	$1.04(\pm0.01)R_\odot$
L	$0.43(\pm0.01)L_\odot$	$1.01(\pm0.02)L_\odot$

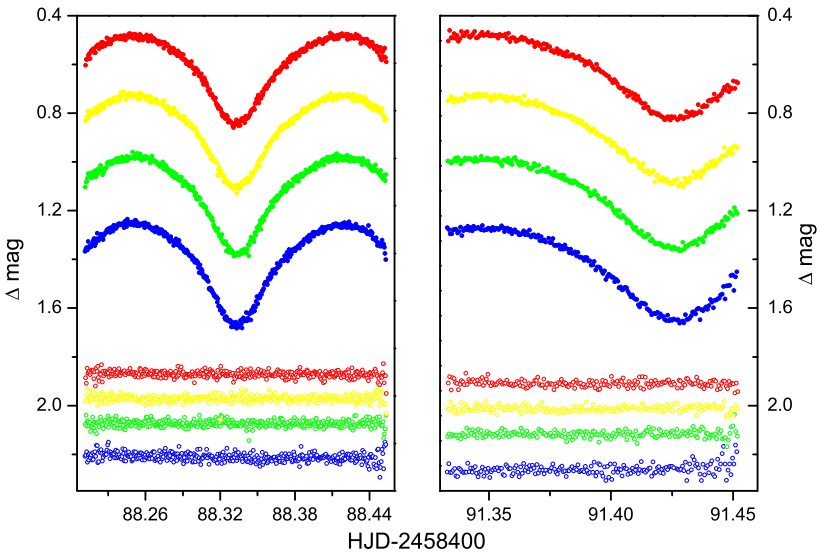

Fig. 1 The light curves obtained on 2019 January 5 are plotted in the left panel of Fig. 1 and the light curves obtained on 2019 January 8 are displayed in the right. The blue, green, yellow and red colors refer to light curves observed with B, V, R_C and I_C filters, respectively. The magnitude differences between the Variable star (OW Leo) and Comparison star (UCAC4 546–051376) are plotted with solid circles and the magnitude differences between the Comparison star (UCAC4 546–051376) and Check star (UCAC4 546–051360) are plotted with open circles.

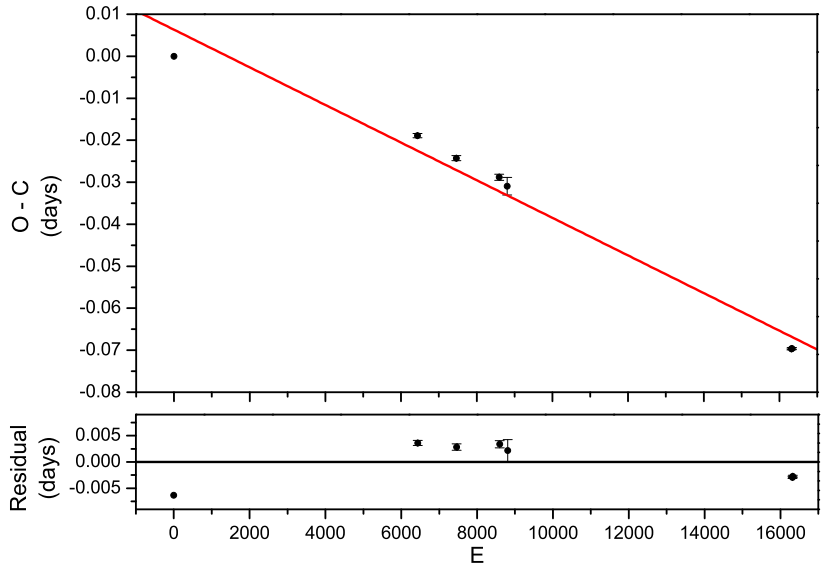

Fig. 2 The black dots in the upper panel refer to observational $O-C$ values calculated from Eq. (1) and the red line represents theoretical $O-C$ curve based on Eq. (2). The fitting residuals are shown in the lower panel of Fig. 2.

4 LIGHT CURVE MODELING

The modeling of OW Leo's light curves have been left out since the eclipsing binary system was discovered. We will model its light curves with the Wilson-Devinney program (Wilson & Devinney 1971). The target have been observed by the LAMOST sky survey project for two times and the low resolution spectra show that OW Leo is a solar-type binary system. The averaged temperature of 5665 K was assumed to the component star. The gravity-darkening coefficients are correspondingly assumed to be $g_1 = g_2 = 0.32$ (Lucy 1967), and the bolometric albedo coefficients

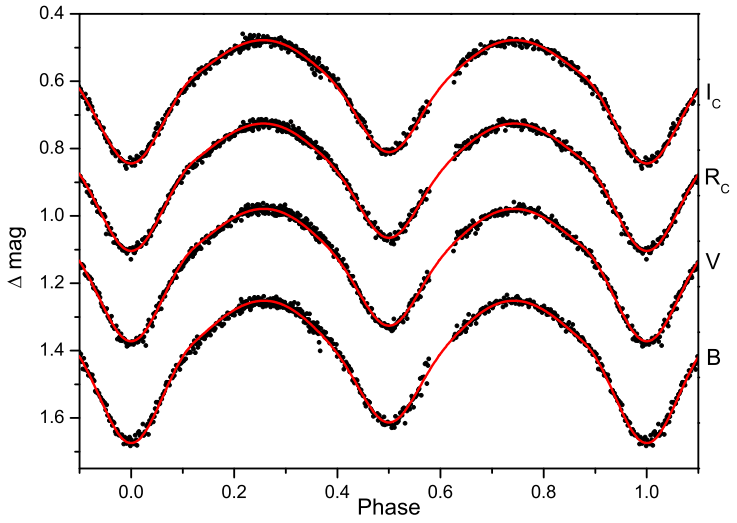

Fig. 3 The black dots are observational light curves obtained with the Xinglong 85cm optical telescope. The red lines are synthetic light curves from the Wilson-Devinney program.

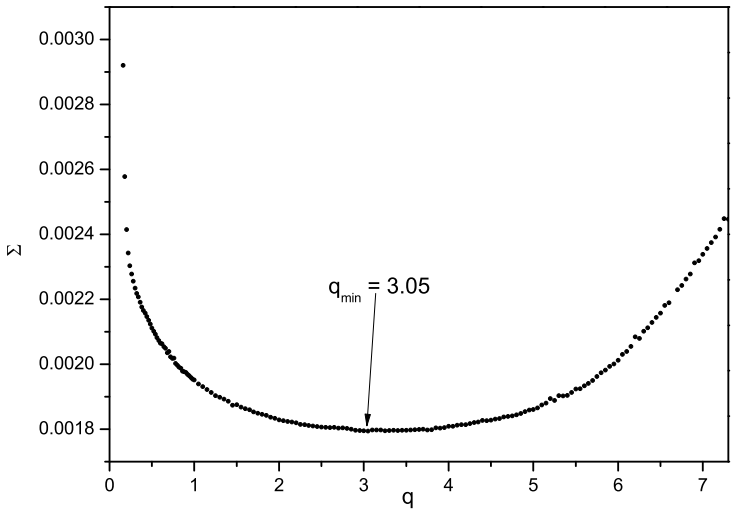

Fig. 4 The q-search diagram.

Table 7 The W-subtype Shallow Contact Binaries

Target	M_1	M_2	R_1	R_2	L_1	L_2	Ref.
V1007 Cas	$0.34M_\odot$	$1.14M_\odot$	$0.69R_\odot$	$1.16R_\odot$	$0.51L_\odot$	$1.44L_\odot$	1
V342 UMa	$0.490M_\odot$	$1.293M_\odot$	$0.766R_\odot$	$1.188R_\odot$	$0.640L_\odot$	$1.303L_\odot$	2
V1197 Her	$0.30M_\odot$	$0.77M_\odot$	$0.54R_\odot$	$0.83R_\odot$	$0.18L_\odot$	$0.38L_\odot$	3
1SWASP J104942.44+141021.5	$0.48M_\odot$	$0.69M_\odot$	$0.60R_\odot$	$0.70R_\odot$	$0.19L_\odot$	$0.23L_\odot$	4
CRTS J145224.5+011522	$0.28M_\odot$	$0.58M_\odot$	$0.44R_\odot$	$0.61R_\odot$	$0.04L_\odot$	$0.08L_\odot$	4
V2790 Ori	$0.33M_\odot$	$1.08M_\odot$	$0.54R_\odot$	$0.91R_\odot$	$0.252L_\odot$	$0.659L_\odot$	5

Reference: (1) Li et al. (2018); (2) Li et al. (2019); (3) Zhou & Soonthornthum (2020); (4) Li et al. (2020); (5) Shokry et al. (2020).

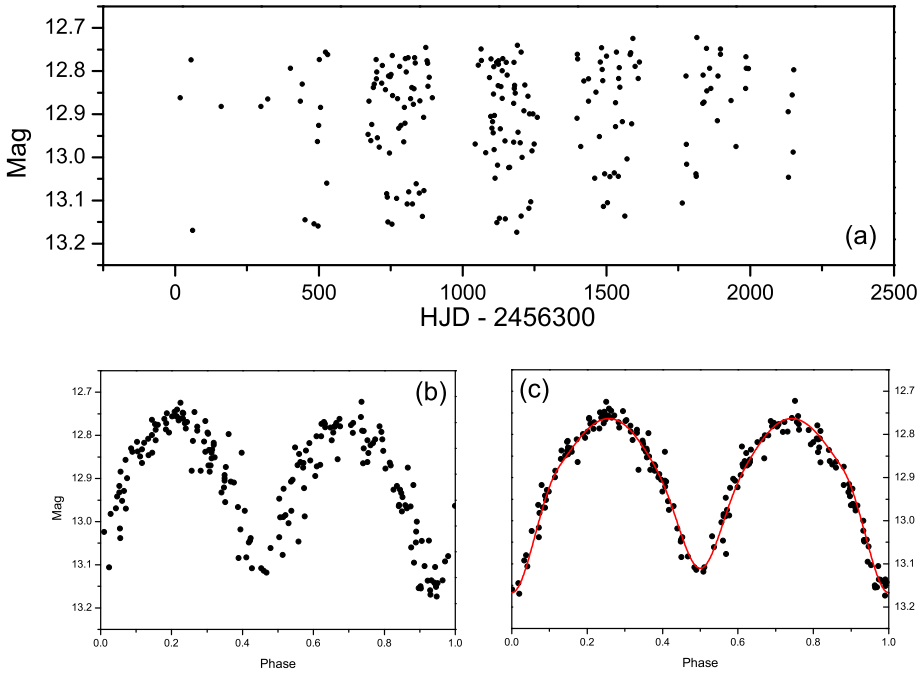

Fig. 5 Observational and synthetic light curves from ASAS-SN.

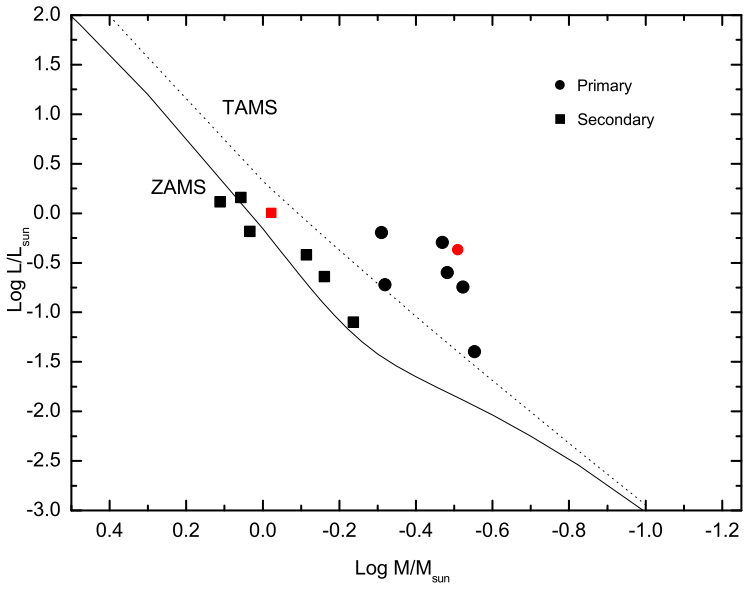

Fig. 6 The H - R diagram. The red circle and square represent the primary and secondary stars in OW Leo.

are assumed to be $A_1 = A_2 = 0.5$ (Ruciński 1969), and the limb darkening coefficients are chosen accordingly (van Hamme 1993). The phased light curves are calculated from the linear ephemeris equation:

$$\mathrm{Min}.I(\mathrm{HJD}) = 2458488.3337 + 0^d.32554052 \times E. \quad (3)$$

4.1 LIGHT CURVES FROM XINGLONG 85CM TELESCOPE

As displayed in Figure 3, the observed light curves are EW-type. Thus, Mode 3 for contact binary, Mode 4 and Mode 5 for semi-contact binary are chosen to modeling the observational light curves. Since there is no radial

velocity curve published, the q-search method is used to get the initial mass ratio (Zhou et al. 2018). Firstly, the temperature of 5665 K was assumed to the primary star (T_2), and the adjustable parameters are orbital inclination (i), modified dimensionless surface potential of the two component stars (Ω_1, Ω_2), mean surface temperature of the secondary star (T_2), bandpass luminosity of the two component stars (L_1, L_2). We then find that the light curves of OW Leo converged in Mode 3 and its mass ratio (M_2/M_1) should be larger than 1, which mean that OW Leo is a W-subtype contact binary system. Therefore, the temperature of 5665K is assumed to the secondary star (T_2). The corresponding q-search diagram are shown in Figure 4. Then, the initial mass ratio is given to be $q = 3.05$ and set as a free parameter to run the Wilson-Devinney program again. Finally, the physical parameter of the binary system are determined, which are listed in Table 5. The synthetic light curves are also plotted in Figure 3. It should be pointed out that we also try to set third light (l_3) as a free parameter, but the light contribution from a tertiary component is not detected.

4.2 LIGHT CURVES FROM ASAS-SN

OW Leo was also observed by the ASAS-SN (Shappee et al. 2014; Jayasinghe et al. 2018) from 2013 January 25 to 2018 November 28. The data from the ASAS-SN was plotted in Figure 5(a). To modeling the data, we converted it to phased light curve. The light curve in Figure 5(b) was calculated based on the original orbital period $P = 0.325545$ days and the light curve in Figure 5(c) was calculated with the corrected orbital period $P = 0.32554052$ days. It is obviously that the orbital period correction is necessary. Then, the phased light curve in Figure 5(c) was also modeled with the Wilson-Devinney program, and the synthetic light curve was plotted with red line in Figure 5(c).

5 DISCUSSION AND CONCLUSIONS

The orbital period and light curves of OW Leo are investigated for the first time, which reveal that its orbital period should be corrected from $P = 0.325545$ days to $P = 0.32554052$ days. According to the photometric results listed in Table 5, we can conclude that OW Leo is a W-subtype shallow contact binary system with its mass ratio to be $q = 3.05(5)$ and fill-out factor to be $f = 12.8(5)\,\%$. The mass of the secondary star is estimated to be $M_2 = 0.95(3)M_\odot$ basing on its effective temperature of $T_2 = 5665$ K (Cox 2000). Then, the other absolute parameters of the two component stars are calculated and listed in Table 6. The orbital semi-major axis is calculated to be $a = 2.15(\pm0.02)R_\odot$ according to the Kepler's third law.

Although research on contact binaries has a very long history, the formation and evolution theories of contact binaries are still incomplete. Webbink (1976) proposed that contact binaries are evolved from initially detached binary systems. The more massive component in a binary system expanded first and filled its critical Roche lobe, and then transfer masses to the less massive companion star through the inner Lagrangian point of the binary system. In recent years, more and more contact binaries have been reported to have additional components orbiting around the central binaries (Yang et al. 2019; Zhou & Soonthornthum 2019; Zhang et al. 2020). The additional components may be ejected from the center of initially multiple star system and pump out angular momentum from the multiple star system, and left out a tight binary system, which will evolve to a contact binary system finally, especially for the formation of M-type contact binaries (Goodwin et al. 2004; Qian et al. 2015). Based on the statistical research of stellar atmospheric parameters of EW-type binaries from the LAMOST, Qian et al. (2019) pointed out that the metal abundance of over $80\,\%$ EW-type binaries are lower than the Sun, which means that they are old population stars. They may evolve from initially detached binary systems through nuclear evolution and angular momentum loss via magnetic braking.

According to the stellar atmospheric parameters in Table 1, we can see that OW Leo is a shallow contact binary with very low metal abundance. Thus, it may have not been contaminated by material from an additional component. It should be evolved from an initially detached binary system through a very long time of main sequence evolution. The absolute parameters of several more W-subtype shallow contact binaries are collected and listed in Table 7. Their evolutionary status is shown in Figure 6. We can see that the less massive stars have already evolved away from the terminal-age main sequence (TAMS), while most of more massive stars are still stay in the main sequence belt. For W-subtype shallow contact binaries, the more massive stars expand and fill the critical Roche lobe on its way evolving to the red giant branch (RGB), and transfer masses to the less evolved component stars. The transferred masses also filled the critical Roche lobe of the less massive star and formed the thin common envelope with the two component star embedded inside. Therefore, the less massive stars seem more evolved than the more massive components.

Acknowledgements This research was supported by the National Natural Science Foundation of China (Grant

Nos. 11703080, 11703082 and 11873017), the Joint Research Fund in Astronomy (Grant No. U1931101) under cooperative agreement between the National Natural Science Foundation of China and Chinese Academy of Sciences, and the Yunnan Fundamental Research Projects (Grant No. 2018FB006). We acknowledge the support of the staff of the Xinglong 85cm telescope. This work was partially supported by the Open Project Program of the Key Laboratory of Optical Astronomy, National Astronomical Observatories, Chinese Academy of Sciences. Guo Shou Jing Telescope (the Large Sky Area Multi-Object Fiber Spectroscopic Telescope LAMOST) is a National Major Scientific Project built by the Chinese Academy of Sciences. Funding for the project has been provided by the National Development and Reform Commission. LAMOST is operated and managed by the National Astronomical Observatories, Chinese Academy of Sciences.

References

Cox, A. N. 2000, Introduction, ed. A. N. Cox, Allen's Astrophysical Quantities (New York: AIP Press; Springer), 1
Cui, X.-Q., Zhao, Y.-H., Chu, Y.-Q., et al. 2012, RAA (Research in Astronomy and Astrophysics), 12, 1197
Diethelm, R. 2010, Information Bulletin on Variable Stars, 5945, 1
Diethelm, R. 2011, Information Bulletin on Variable Stars, 5992, 1
Diethelm, R. 2012, Information Bulletin on Variable Stars, 6029, 1
Goodwin, S. P., Whitworth, A. P., & Ward-Thompson, D. 2004, A&A, 414, 633
He, J.-j., & Wang, J.-j. 2019, Advances in Astronomy, 2019, 5641518
Jayasinghe, T., Kochanek, C. S., Stanek, K. Z., et al. 2018, MNRAS, 477, 3145
Li, K., Xia, Q. Q., Hu, S. M., et al. 2018, PASP, 130, 074201
Li, K., Xia, Q.-Q., Liu, J.-Z., et al. 2019, RAA (Research in Astronomy and Astrophysics), 19, 147
Li, K., Kim, C.-H., Xia, Q.-Q., et al. 2020, AJ, 159, 189
Liu, L., Qian, S. B., & Xiong, X. 2018, MNRAS, 474, 5199
Lucy, L. B. 1967, ZAp, 65, 89
Pi, Q.-f., Zhang, L.-y., Bi, S.-l., et al. 2017, AJ, 154, 260
Qian, S. B., Jiang, L. Q., Fernández Lajús, E., et al. 2015, ApJL, 798, L42
Qian, S.-B., He, J.-J., Zhang, J., et al. 2017, RAA (Research in Astronomy and Astrophysics), 17, 087
Qian, S. B., Zhang, J., He, J. J., et al. 2018, ApJS, 235, 5
Qian, S.-B., Shi, X.-D., Zhu, L.-Y., et al. 2019, RAA (Research in Astronomy and Astrophysics), 19, 064
Ruciński, S. M. 1969, Acta Astronomica, 19, 245
Shappee, B. J., Prieto, J. L., Grupe, D., et al. 2014, ApJ, 788, 48
Shokry, A., Zead, I. Z., El-Depsey, M. H., et al. 2020, New Astron., 80, 101400
Tody, D. 1986, in SPIE Conference Series, 627, Instrumentation in astronomy VI, ed. D. L. Crawford, 733
van Hamme, W. 1993, AJ, 106, 2096
Watson, C. L., Henden, A. A., & Price, A. 2006, Society for Astronomical Sciences Annual Symposium, 25, 47
Webbink, R. F. 1976, ApJS, 32, 583
Wilson, R. E., & Devinney, E. J. 1971, ApJ, 166, 605
Yang, Y., Yuan, H., & Dai, H. 2019, AJ, 157, 111
Zhang, B., Qian, S.-B., Michel, R., et al. 2018a, RAA (Research in Astronomy and Astrophysics), 18, 030
Zhang, B., Qian, S.-B., Wang, J.-J., et al. 2020, RAA (Research in Astronomy and Astrophysics), 20, 047
Zhang, X., Wu, J., & Meng, N. 2018b, MNRAS, 478, 3513
Zhao, G., Zhao, Y.-H., Chu, Y.-Q., Jing, Y.-P., & Deng, L.-C. 2012, RAA (Research in Astronomy and Astrophysics), 12, 723
Zhou, A.-Y., Jiang, X.-J., Zhang, Y.-P., & Wei, J.-Y. 2009, RAA (Research in Astronomy and Astrophysics), 9, 349
Zhou, X., Qian, S., Boonrucksar, S., et al. 2018, PASJ, 70, 87
Zhou, X., & Soonthornthum, B. 2019, PASJ, 71, 39
Zhou, X., & Soonthornthum, B. 2020, RAA (Research in Astronomy and Astrophysics), 20, 010